Three-Mode Interactions in Harmonically Excited Systems with Quadratic Nonlinearities

T. A. NAYFEH

Department of Mechanical Engineering and Industrial Engineering, University of Illinois at Urbana-Champaign, Urbana, IL 61801, U.S.A.

W. ASRAR

Department of Mechanical Engineering, Aligarh Muslim University, Aligarh 202 002, India

and

A. H. NAYFEH

Department of Engineering Science and Mechanics, Virginia Polytechnic Institute and State University, Blacksburg, VA 24061, U.S.A.

(Received: 16 September 1991; accepted: 18 November 1991)

Abstract. An investigation is presented of the response of a three-degree-of-freedom system with quadratic nonlinearities and the autoparametric resonances $\omega_3 \approx 2\omega_2$ and $\omega_2 \approx 2\omega_1$ to a harmonic excitation of the third mode, where the ω_m are the linear natural frequencies of the system. The method of multiple scales is used to determine six first-order nonlinear ordinary differential equations that govern the time variation of the amplitudes and phases of the interacting modes. The fixed points of these equations are obtained and their stability is determined. For certain parameter values, the fixed points are found to lose stability due to Hopf bifurcations and consequently the system exhibits amplitude- and phase-modulated motions. Regions where the amplitudes and phases display periodic, quasiperiodic, and chaotic time variations and hence regions where the overall system motion is periodically, quasiperiodically, and chaotically modulated are determined. Using various numerical simulations, we investigated nonperiodic solutions of the modulation equations using the amplitude F of the excitation as a control parameter. As the excitation amplitude F is increased, the fixed points of the modulation equations exhibit an instability due to a Hopf bifurcation, leading to limit-cycle solutions of the modulation equations. As F is increased further, the limit cycle undergoes a period-doubling bifurcation followed by a secondary Hopf bifurcation, resulting in either a two-period quasiperiodic or a phase-locked solution. As F is increased further, there is a torus breakdown and the solution of the modulation equations becomes chaotic, resulting in a chaotically modulated motion of the system.

Key words: Autoparametric resonance, torus, chaos, Hopf bifurcation.

1. Introduction

Lefschetz [1] described a commercial airplane in which the propellers induced a vibration of order one-half in the wings, which in turn induced a subharmonic vibration of order one-fourth in the rudder. The oscillations were so violent that the airplane broke up. This motivated us to consider the response of a three-degree-of-freedom system with quadratic nonlinearities to a primary excitation. The motion of the system is governed by the three coupled second-order nonlinear ordinary differential equations

Nonlinear Dynamics **3**: 385–410, 1992.

$$\ddot{u}_1 + \omega_1^2 u_1 + 2\varepsilon\mu_1\dot{u}_1 = \varepsilon \frac{\partial V}{\partial u_1} \tag{1}$$

$$\ddot{u}_2 + \omega_2^2 u_2 + 2\varepsilon\mu_2\dot{u}_2 = \varepsilon \frac{\partial V}{\partial u_2} \tag{2}$$

$$\ddot{u}_3 + \omega_3^2 u_3 + 2\varepsilon\mu_3\dot{u}_3 = \varepsilon \frac{\partial V}{\partial u_3} + \varepsilon f \cos \Omega t\,, \tag{3}$$

where

$$V = \alpha_1 u_1^3 + \alpha_2 u_1^2 u_2 + \alpha_3 u_1 u_2^2 + \alpha_4 u_1^2 u_3 + \alpha_5 u_1 u_3^2 + \alpha_6 u_2^3 + \alpha_7 u_2^2 u_3 + \alpha_8 u_2 u_3^2 + \alpha_9 u_3^3 + \alpha_{10} u_1 u_2 u_3 \tag{4}$$

and the ω_n, α_n, f, Ω, and μ_n are constants and the dots represent time derivatives. Here, ε is a small dimensionless parameter used for bookkeeping and can be set equal to one in the final solution. We consider the case of simultaneous internal (autoparametric) resonances of the type $\omega_3 \approx 2\omega_2$ and $\omega_2 \approx 2\omega_1$. In these equations, we can think of u_3 to represent the motion of the propellers, u_2 to represent the motion of the wing, and u_1 to represent the motion of the rudder.

The responses of nonlinear systems to harmonic excitations often exhibit complicated long-time behaviors when their natural frequencies are commensurable [2, 3]; that is, when the system has an internal or autoparametric resonance. For example, in 1863 Froude [4] observed that a ship whose pitch frequency is twice its roll frequency has undesirable seakeeping characteristics. The explanation cannot be found in the linearized equations governing the motion of the ship because the yaw, sway, and roll modes are not coupled with the pitch, heave, and surge modes.

Mettler and Weidenhammer [5], Sethna [6], and Haxton and Barr [7] used the method of averaging to analyze primary resonances of systems governed by equations with quadratic nonlinearities when one natural frequency is twice another. Nayfeh, Mook, and Marshall [8] used the method of multiple scales [9, 10] to analyze a simple system of two coupled oscillators with quadratic nonlinearities as a model for the coupled pitch and roll motions of ships. They investigated primary resonances of both the first and second modes. When $\omega_2 \approx 2\omega_1$ and $\Omega \approx \omega_2$, where Ω is the excitation frequency, and the ω_j are the linear natural frequencies, they found a saturation phenomenon. Moreover, when $\omega_2 \approx 2\omega_1$ and $\Omega \approx \omega_1$, they showed that there are conditions for which stable periodic steady-state motions do not exist. Instead, there exist amplitude- and phase-modulated motions in which the energy is continuously exchanged between the two modes.

Later, Yamamoto and co-workers [11, 12] used the method of harmonic balance and analog-computer simulations to investigate the forced responses of systems with quadratic and cubic nonlinearities to harmonic excitations when one natural frequency is twice another. They observed amplitude- and phase-modulated steady-state motions in their analog-computer simulations when $\Omega \approx \omega_2$ and $\Omega \approx \omega_1$. Nayfeh and Mook [13] used the method of multiple scales to analyze the response of a beam to a harmonic excitation. They accounted for a two-to-one autoparametric resonance between a lateral mode and a longitudinal mode. Hatwal, Mallik, and Ghosh [14] reported analytical and numerical results for the response of two internally resonant

coupled oscillators to a harmonic excitation when the excitation frequency Ω is near ω_2. Their results for small amplitudes are equivalent to those of Sethna [6] and Nayfeh *et al.* [8]. However, their numerical results for sufficiently large amplitudes show that periodic responses are unstable and give way to periodically modulated motions. Miles [15] used the method of averaging to investigate the response of two internally resonant, quadratically coupled oscillators to harmonic excitations. He examined the stability of the analytical solutions and investigated the possible bifurcations. He presented numerical results that demonstrate chaotically and periodically modulated motions when the excitation frequency Ω is near the lower natural frequency ω_1. Nayfeh and Raouf [16, 17] used the method of multiple scales to investigate the response of a circular cylindrical shell to a harmonic internal pressure when the natural frequency ω_2 of the breathing mode is twice the natural frequency ω_1 of a flexural mode. They also found the saturation phenomenon when $\Omega \approx \omega_2$ and presented numerical results that demonstrate chaotically and periodically modulated motions. Nayfeh [18] used the method of multiple scales to analyze the pitch and roll motion of a ship subject to a primary-resonant excitation. He found conditions for the existence of amplitude- and phase-modulated motions.

Hatwal, Mallik, and Ghosh [19] reported experimental data and numerical results that demonstrate chaotic motions. Haddow, Barr, and Mook [20] conducted an experiment using a two-degree-of-freedom model consisting of two light-weight beams and two concentrated masses and observed the saturation phenomenon when $\Omega \approx \omega_2$ and the nonexistence of periodic steady-state motions when $\Omega \approx \omega_1$. Using a model similar to that of Haddow *et al.* [20], Nayfeh and Zavodney [21] observed amplitude- and phase-modulated motions when $\Omega \approx \omega_1$. Nayfeh *et al.* [22], Nayfeh and Balachandran [23], and Balachandran and Nayfeh [24, 25] performed experimental studies on metallic and composite structures with quadratic nonlinearities and a two-to-one internal resonance. They observed periodically and chaotically modulated motions when $\Omega \approx \omega_2$.

Mook, Marshall, and Nayfeh [26] analyzed the cases of subharmonic and superharmonic resonances in the pitch and roll motions of ships. Mook and co-workers [27, 28] used the method of multiple scales to investigate the influence of a two-to-one internal resonance on the response of a system with quadratic nonlinearities to a combination resonance (i.e., $\Omega \approx \omega_2 + \omega_1$) and a subharmonic resonance of the higher mode (i.e., $\Omega \approx 2\omega_2$). They applied the results to an arch and found that the internal resonance significantly reduces the response. Balachandran and Nayfeh [29] experimentally investigated subharmonic and combination resonant excitations of internally resonant metallic and composite structures.

All of the previously mentioned works dealt with a single internal resonance of the two-to-one type. Nayfeh and Mook [30] investigated the response of a three-degree-of-freedom system with the combination internal resonance $\omega_3 \approx \omega_2 + \omega_1$. They demonstrated the existence of the saturation phenomenon when the higher mode is excited by a primary resonance; that is, $\Omega \approx \omega_3$. Ibrahim and Barr [31] investigated the response of a fluid-filled circular container resting on a vibrating structure with an autoparametric coupling involving the first antisymmetric liquid sloshing mode and two orthogonal structural modes. Ibrahim, Woodall, and Heo [32] investigated the response of a three-degree-of freedom structure with the internal resonant condition $\omega_j \approx |\omega_j \pm \omega_k|$. They found that the system achieves a "quasi-steady response" and exhibits an energy exchange between the directly excited mode and the two indirectly excited modes. Bux and Roberts [33] and Nayfeh, Nayfeh, and Mook [34] theoretically and experimentally investigated the primary resonant response of a structure exhibiting an autoparametric combination resonance of the additive type. They demonstrated the saturation phenomenon. Ashworth and Barr [35] investigated theoretically and experimentally the response of a model of a fuselage and T-tail of an

aircraft. The system was idealized as a lumped mass four-degree-of-freedom system having four masses and three beams. They considered the resonant case $\omega_4 = \omega_3 + \omega_1$ and $\Omega = \omega_2 + \omega_4$.

Sridhar, Mook, and Nayfeh [36] and Hadian and Nayfeh [37] studied the response of a circular plate with $\omega_1 + 2\omega_2 \approx \omega_3$ (essentially a three-degree-of-freedom problem). When $\Omega \approx \omega_3$, Hadian and Nayfeh [37] found that the equations describing the amplitudes and phases of the interacting modes possess periodic solutions that undergo a period-doubling sequence leading to chaos.

Bux and Roberts [33] and Cartmell and Roberts [38] investigated the response of a structure that consists of two beams and one mass. The first beam is a cantilever mounted in the horizontal direction and the second beam is vertically mounted at the end of the first but is rotated so that its transverse vibrations occur out of plane with respect to the horizontal beam (essentially a four-degree-of-freedom structure). Bux and Roberts [33] studied the effect of simultaneous combination and two-to-one internal resonances; that is, $\omega_2 \approx \omega_B + \omega_T$ and $\omega_1 \approx 2\omega_B$, where ω_1 and ω_2 are the frequencies of the first and second in-plane bending modes of the first beam, ω_B is the frequency of the first out-of-plane bending mode of the second beam, and ω_T is the torsional frequency of the mass and the second beam. They found that the large-amplitude motion of the directly excited mode can be absorbed by the modes that are excited through the internal resonance. Balachandran and Nayfeh [24, 29] experimentally studied the response of a three-degree-of-freedom composite structure with two light-weight composite beams and two concentrated masses. The structure possesses the two internal resonances $\omega_2 \approx 3\omega_1$ and $\omega_2 \approx 2\omega_t$, where ω_1 and ω_2 are the frequencies of the first two bending modes and ω_t is the frequency of the first torsional mode. When the lower bending mode was excited by a primary resonance, they found that, for a small excitation amplitude F, the response is periodic consisting of only the excited mode. As F exceeded a threshold value, the single-mode response lost stability, giving way to a periodic response consisting of the two bending modes. As F exceeded a second threshold value, the two-mode response lost stability to a periodic response consisting of the torsional mode as well as the two bending modes. Fujino, Pacheco, and Warnitchai [39] investigated experimentally and analytically the response of a cable-stayed-beam model having three frequencies in the ratio 1:1:2 to a harmonic excitation of the higher mode. They demonstrated the saturation phenomenon.

Ibrahim [40] considered the case when $\omega_3 \approx 2\omega_2$, $\omega_2 \approx 2\omega_1$, and $\Omega \approx \omega_3$ for a general three-degree-of-freedom system. He used the method of multiple scales to determine the equations describing the amplitudes and phases of the interacting modes. He determined the fixed points and ascertained their stability using the Routh–Hurwitz criterion. He did not identify any Hopf bifurcations and consequently did not study any nonperiodic motions. Tadjbakhsh and Wang [41] investigated the response of wind-driven cables. They modeled the cable as a three-degree-of freedom system with quadratic nonlinearities with the internal resonant conditions $\omega_3 \approx 2\omega_2$ and $\omega_2 \approx 2\omega_1$. They considered the case when the second mode is excited (i.e., $\Omega \approx \omega_2$) and found that the system exhibits both the saturation and jump phenomena.

The objective of this work is to study the behavior of a three-degree-of-freedom system with quadratic nonlinearities in the restoring and/or inertial force terms. The case of internal resonant conditions $\omega_3 \approx 2\omega_2$ and $\omega_2 \approx 2\omega_1$ is considered. Our goal is to study the long-time behavior of the system. The method of multiple time scales is used to obtain the equations that govern the amplitudes and phases. The bifurcations of the fixed points of these equations include Hopf bifurcations. Using various numerical simulations, we show that these equations possess complicated solutions, such as periodic, two-period quasiperiodic, and chaotic solutions. The phase-locking phenomenon is also demonstrated.

2. Method of Solution: Multiple Scales

We seek a first-order uniform expansion of the solution of equations (1)–(4) in the form

$$u_n(t;\varepsilon) = u_{no}(T_0, T_1) + \varepsilon u_{n1}(T_0, T_1) + \cdots \tag{5a}$$

where $T_0 = t$ is a fast scale associated with changes occurring at the frequencies Ω and ω_n, and $T_1 = \varepsilon t$ is a slow scale associated with the modulations of the amplitudes and phases due to the nonlinearities, damping, and resonances. The first- and second-order time derivatives transform as

$$\frac{\mathrm{d}}{\mathrm{d}t} = D_0 + \varepsilon D_1 + \cdots, \qquad \text{and} \qquad \frac{\mathrm{d}^2}{\mathrm{d}t^2} = D_0^2 + 2\varepsilon D_0 D_1 + \cdots \tag{5b}$$

where $D_n = \partial/\partial T_n$. Substituting equations (5) into equations (1)–(4) and equating coefficients of like powers of ε, one obtains

Order ε^0:

$$D_0^2 u_{10} + \omega_1^2 u_{10} = 0\,, \tag{6}$$

$$D_0^2 u_{20} + \omega_2^2 u_{20} = 0\,, \tag{7}$$

$$D_0^2 u_{30} + \omega_3^2 u_{30} = 0\,. \tag{8}$$

Order ε:

$$\begin{aligned} D_0^2 u_{11} + \omega_1^2 u_{11} = {} & -2D_0 D_1 u_{10} - 2\mu_1 D_0 u_{10} + 3\alpha_1 u_{10}^2 + 2\alpha_2 u_{10} u_{20} \\ & + \alpha_3 u_{20}^2 + 2\alpha_4 u_{10} u_{30} + \alpha_5 u_{30}^2 + \alpha_{10} u_{20} u_{30}\,, \end{aligned} \tag{9}$$

$$\begin{aligned} D_0^2 u_{21} + \omega_2^2 u_{21} = {} & -2D_0 D_1 u_{20} - 2\mu_2 D_0 u_{20} + \alpha_2 u_{10}^2 + 2\alpha_3 u_{10} u_{20} \\ & + 3\alpha_6 u_{20}^2 + 2\alpha_7 u_{20} u_{30} + \alpha_8 u_{30}^2 + \alpha_{10} u_{10} u_{30}\,, \end{aligned} \tag{10}$$

$$\begin{aligned} D_0^2 u_{31} + \omega_3^2 u_{31} = {} & -2D_0 D_1 u_{30} - 2\mu_3 D_0 u_{30} + \alpha_4 u_{10}^2 + 2\alpha_5 u_{10} u_{30} \\ & + \alpha_7 u_{20}^2 + 2\alpha_8 u_{20} u_{30} + 3\alpha_9 u_{30}^2 + \alpha_{10} u_{10} u_{20} + f\cos\Omega T_0\,. \end{aligned} \tag{11}$$

The general solutions of equations (6)–(8) can be expressed in the form

$$u_{no} = A_n(T_1)\exp(i\omega_n T_0) + cc \tag{12}$$

for $n = 1$, 2, and 3, where cc denotes the complex conjugate of the preceding terms, and the A_n are to be determined through the elimination of secular and small-divisor terms from the next-order equations. In this paper, we analyze the case $\omega_3 \approx 2\omega_2$, $\omega_2 \approx 2\omega_1$, and $\Omega \approx \omega_3$.

Substituting equations (12) into equations (9)–(11) and recalling the resonances being studied, we obtain

$$D_0^2 u_{11} + \omega_1^2 u_{11} = -2i\omega_1(A_1' + \mu_1 A_1)e^{i\omega_1 T_0} + 2\alpha_2 A_2 \bar{A}_1 e^{i(\omega_2-\omega_1)T_0} + cc + NST\,, \tag{13}$$

$$D_0^2 u_{21} + \omega_2^2 u_{21} = -2i\omega_2(A_2' + \mu_2 A_2)e^{i\omega_2 T_0} + \alpha_2 A_1^2 e^{2i\omega_1 T_0} + 2\alpha_7 A_3 \bar{A}_2 e^{i(\omega_3-\omega_2)T_0} + cc + NST\,, \tag{14}$$

$$D_0^2 u_{31} + \omega_3^2 u_{31} = -2i\omega_3(A_3' + \mu_3 A_3)e^{i\omega_3 T_0} + \alpha_7 A_2^2 e^{2i\omega_2 T_0} + f\cos\Omega T_0 + cc + NST\,, \tag{15}$$

where the overbar indicates the complex conjugate, the prime indicates differentiation with respect to T_1, and NST stands for terms that do not produce secular or small-divisor terms. To describe quantitatively the nearness of the resonances, we introduce the detuning parameters σ, σ_2, and σ_3 according to

$$\omega_2 = 2\omega_1 + \varepsilon\sigma_2, \quad \omega_3 = 2\omega_2 + \varepsilon\sigma_3, \quad \Omega = \omega_3 + \varepsilon\sigma\,. \tag{16}$$

Substituting equations (16) into equations (13)–(15) and eliminating the secular terms from u_{11}, u_{21}, and u_{31}, one obtains

$$-2i\omega_1(A_1' + \mu_1 A_1) + 2\alpha_2 A_2 \bar{A}_1 e^{i\sigma_2 T_1} = 0\,, \tag{17}$$

$$-2i\omega_2(A_2' + \mu_2 A_2) + \alpha_2 A_1^2 e^{-i\sigma_2 T_1} + 2\alpha_7 A_3 \bar{A}_2 e^{i\sigma_3 T_1} = 0\,, \tag{18}$$

$$-2i\omega_3(A_3' + \mu_3 A_3) + \alpha_7 A_2^2 e^{-i\sigma_3 T_1} + \frac{1}{2} f e^{i\sigma T_1} = 0\,. \tag{19}$$

Expressing the A_n in the polar form

$$A_1 = \frac{\sqrt{2\omega_1\omega_2}}{\alpha_2} a_1 e^{i\beta_1}\,, \quad A_2 = \frac{\omega_1}{\alpha_2} a_2 e^{i\beta_2}\,, \quad \text{and } A_3 = \frac{\omega_2}{\alpha_7} a_3 e^{i\beta_3} \tag{20}$$

and separating equations (17)–(19) into real and imaginary parts yields the modulation equations

$$a_1' = -\mu_1 a_1 + a_1 a_2 \sin\gamma_1 \tag{21}$$

$$a_2' = -\mu_2 a_2 - a_1^2 \sin\gamma_1 + a_2 a_3 \sin\gamma_2 \tag{22}$$

$$a_3' = -\mu_3 a_3 - \Gamma a_2^2 \sin\gamma_2 + F\sin\gamma_3 \tag{23}$$

$$a_1\beta_1' = -a_1 a_2 \cos\gamma_1 \tag{24}$$

$$a_2\beta_2' = -a_1^2 \cos\gamma_1 - a_2 a_3 \cos\gamma_2 \tag{25}$$

$$a_3\beta_3' = -\Gamma a_2^2 \cos\gamma_2 - F\cos\gamma_3\,, \tag{26}$$

where

$$\gamma_1 = \beta_2 - 2\beta_1 + \sigma_2 T_1\,, \quad \gamma_2 = \beta_3 - 2\beta_2 + \sigma_3 T_1\,, \quad \gamma_3 = \sigma T_1 - \beta_3\,, \tag{27}$$

$$\Gamma = \omega_1^2 \alpha_7^2 / 2\omega_2 \omega_3 \alpha_2^2 , \quad F = f\alpha_7 / 4\omega_2 \omega_3 . \tag{28}$$

Equations (21)–(27) constitute a sixth-order dimensional system for the six state variables a_1, a_2, a_3, γ_1, γ_2, and γ_3 and the eight control parameters μ_1, μ_2, μ_3, σ, σ_2, σ_3, Γ, and F. In what follows, we study solutions of these equations using the amplitude F of the excitation and the detuning σ of the primary resonance (essentially the frequency of the excitation) as control parameters.

Solving equations (27) for the β_n yields

$$\beta_3 = \sigma T_1 - \gamma_3 , \quad \beta_2 = \frac{1}{2}(\sigma + \sigma_3) T_1 - \frac{1}{2}\gamma_2 - \frac{1}{2}\gamma_3 ,$$

$$\beta_1 = \frac{1}{4}(\sigma + 2\sigma_2 + \sigma_3) T_1 - \frac{1}{4}(2\gamma_1 + \gamma_2 + \gamma_3) . \tag{29}$$

Substituting equations (29) into equations (20), using equations (16), and substituting the result into equations (5a) and (12), we obtain to the first approximation

$$u_1 \approx \frac{2\sqrt{2\omega_1 \omega_2}}{\alpha_2} a_1 \cos\left[\frac{1}{4}(\Omega t - 2\gamma_1 - \gamma_2 - \gamma_3)\right] \tag{30}$$

$$u_2 \approx \frac{2\omega_1}{\alpha_2} a_2 \cos\left[\frac{1}{2}(\Omega t - \gamma_2 - \gamma_3)\right] \tag{31}$$

$$u_3 \approx \frac{2\omega_2}{\alpha_7} a_3 \cos(\Omega t - \gamma_3) , \tag{32}$$

where the a_n and γ_n are given by equations (21)–(27).

3. Periodic Motions

It follows from equations (30)–(32) that constant a_n and γ_n correspond to periodic responses, which in turn correspond to the fixed points or constant solutions of equations (21)–(27). It follows from equations (29) that

$$\beta_1' = \frac{1}{4}(\sigma + 2\sigma_2 + \sigma_3) = \nu_1 , \quad \beta_2' = \frac{1}{2}(\sigma + \sigma_3) = \nu_2 , \quad \beta_3' = \sigma = \nu_3 . \tag{33}$$

Hence, the fixed points or constant solutions of equations (21)–(27) are given by

$$-\mu_1 a_1 + a_1 a_2 \sin \gamma_1 = 0 \tag{34}$$

$$-\mu_2 a_2 - a_1^2 \sin \gamma_1 + a_2 a_3 \sin \gamma_2 = 0 \tag{35}$$

$$-\mu_3 a_3 - \Gamma a_2^2 \sin \gamma_2 + F \sin \gamma_3 = 0 \tag{36}$$

$$\nu_1 a_1 = -a_1 a_2 \cos \gamma_1 \tag{37}$$

$$\nu_2 a_2 = -a_1^2 \cos \gamma_1 - a_2 a_3 \cos \gamma_2 \tag{38}$$

$$\sigma a_3 = -\Gamma a_2^2 \cos \gamma_2 - F \cos \gamma_3 . \tag{39}$$

There are three possibilities: (*a*) $a_1 = 0$, $a_2 = 0$, and $a_3 \neq 0$; (*b*) $a_1 = 0$, $a_2 \neq 0$, and $a_3 \neq 0$; and (c) $a_1 \neq 0$, $a_2 \neq 0$, and $a_3 \neq 0$.

Case (*a*).
In this case, $a_1 = a_2 = 0$ and

$$a_3 = \frac{F}{\sqrt{\sigma^2 + \mu_3^2}} \tag{40}$$

and hence $u_1 = u_2 = 0$ and

$$u_3 \approx \frac{2\omega_2}{\alpha_7} a_3 \cos(\Omega t - \gamma_3) \tag{41}$$

which is essentially the linear solution.

Case (*b*).
In this case, $a_1 = 0$,

$$a_3 = (\mu_2^2 + \nu_2^2)^{1/2} \tag{42}$$

and

$$\Gamma a_2^2 = -(\mu_2 \mu_3 - \sigma \nu_2) \pm [F - (\mu_3 \nu_2 + \sigma \mu_2)^2]^{1/2} . \tag{43}$$

Hence,

$$u_1 \approx 0 , \quad u_2 \approx \frac{2\omega_1}{\alpha_2} a_2 \cos\left[\frac{1}{2}(\Omega t - \gamma_2 - \gamma_3)\right] \tag{44}$$

and

$$u_3 \approx \frac{2\omega_2}{\alpha_7} a_3 \cos(\Omega t - \gamma_3) . \tag{45}$$

Case (*c*).
In this case,

$$a_2 = (\mu_1^2 + \nu_1^2)^{1/2} \tag{46}$$

$$a_1^2 = -\chi_1 \pm \sqrt{\chi_1^2 - \chi_2} \tag{47}$$

$$(\mu_3^2 + \sigma^2) a_3^2 = F^2 - 2\Gamma(\mu_3 \mu_1 + \sigma \nu_1) a_1^2 - 2\Gamma(\mu_2 \mu_3 - \sigma \nu_2) a_2^2 - \Gamma^2 a_2^4 \tag{48}$$

where

$$\chi_1 = \left[\mu_1\mu_2 - \nu_1\nu_2 + \frac{a_2^2}{\mu_3^2 + \sigma^2} (\mu_3\mu_1 + \sigma\nu_1) \right] \tag{49}$$

$$\chi_2 = (\mu_2^2 + \nu_2^2)a_2^2 - \frac{a_2^2}{\mu_3^2 + \sigma^2} [F^2 - 2\Gamma(\mu_2\mu_3 - \sigma\nu_2)a_2^2 + \Gamma^2 a_2^4] \tag{50}$$

and the response is given by equations (30)–(32).

4. Stability of the Fixed Points

To analyze the stability of the fixed points of equations (21)–(27), we let

$$A_1 = \frac{\sqrt{2\omega_1\omega_2}}{\alpha_2} (p_1 - iq_1)e^{i\nu_1 T_1}, \quad A_2 = \frac{\omega_1}{\alpha_2} (p_2 - iq_2)e^{i\nu_2 T_1}, \quad \text{and } A_3 = \frac{\omega_2}{\alpha_7} (p_3 - iq_3)e^{i\nu_3 T_1}, \tag{51}$$

where the p_n and q_n are real and the ν_n are defined in equations (33). Substituting equations (51) into equations (17)–(19) and separating real and imaginary parts, one obtains

$$p_1' + \mu_1 p_1 + \nu_1 q_1 + p_1 q_2 - p_2 q_1 = 0 \tag{52}$$

$$q_1' + \mu_1 q_1 - \nu_1 p_1 - p_1 p_2 - q_1 q_2 = 0 \tag{53}$$

$$p_2' + \mu_2 p_2 + \nu_2 q_2 + 2p_1 q_1 + p_2 q_3 - p_3 q_2 = 0 \tag{54}$$

$$q_2' + \mu_2 q_2 - \nu_2 p_2 - p_1^2 + q_1^2 - p_2 p_3 - q_2 q_3 = 0 \tag{55}$$

$$p_3' + \mu_3 p_3 + \nu_3 q_3 + 2\Gamma p_2 q_2 = 0 \tag{56}$$

$$q_3' + \mu_3 q_3 - \nu_3 p_3 - \Gamma(p_2^2 - q_2^2) - F = 0 . \tag{57}$$

In this case, the state variables are p_m and q_m, $m = 1, 2$ and 3, and the control parameters are Γ, F, and μ_m and ν_m, $m = 1, 2$, and 3. We note that these equations are invariant under the transformations

$$p_1 \to -p_1,\ q_1 \to -q_1,\ p_2 \to p_2,\ q_2 \to q_2,\ p_3 \to p_3,\ q_3 \to q_3 \tag{58}$$

$$p_1 \to q_1,\ q_1 \to -p_1,\ p_2 \to -p_2,\ q_2 \to -q_2,\ p_3 \to p_3,\ q_3 \to q_3 \tag{59}$$

$$p_1 \to -q_1,\ q_1 \to p_1,\ p_2 \to -p_2,\ q_2 \to -q_2,\ p_3 \to p_3,\ q_3 \to q_3 . \tag{60}$$

Substituting equations (51) into equations (12) and using equations (16) and (33), we find that to the first approximation

$$u_1 \approx \frac{2\sqrt{2\omega_1\omega_2}}{\alpha_2}\left[p_1\cos\left(\frac{1}{4}\Omega t\right) + q_1\sin\left(\frac{1}{4}\Omega t\right)\right] \tag{61}$$

$$u_2 \approx \frac{2\omega_1}{\alpha_2}\left[p_2\cos\left(\frac{1}{2}\Omega t\right) + q_2\sin\left(\frac{1}{2}\Omega t\right)\right] \tag{62}$$

$$u_3 \approx \frac{2\omega_2}{\alpha_7}\left[p_3\cos(\Omega t) + q_3\sin(\Omega t)\right] \tag{63}$$

where the p_i and q_i are given by equations (52)–(57).

The stability of a particular fixed point with respect to perturbations proportional to $\exp(\lambda T_1)$ depends on the real parts of the roots of the characteristic equation

$$\begin{vmatrix} \lambda+\mu_1+q_2 & \nu_1-p_2 & -q_1 & p_1 & 0 & 0 \\ -\nu_1-p_2 & \lambda+\mu_1-q_2 & -p_1 & -q_1 & 0 & 0 \\ 2q_1 & 2p_1 & \lambda+\mu_2+q_3 & \nu_2-p_3 & -q_2 & p_2 \\ -2p_1 & 2q_1 & -\nu_2-p_3 & \lambda+\mu_2-q_3 & -p_2 & -q_2 \\ 0 & 0 & 2\Gamma q_2 & 2\Gamma p_2 & \lambda+\mu_3 & \nu_3 \\ 0 & 0 & -2\Gamma p_2 & 2\Gamma q_2 & -\nu_3 & \lambda+\mu_3 \end{vmatrix} = 0 . \tag{64}$$

Thus, a fixed point given by equations (46)–(48) is asymptotically stable if and only if the real parts of all the roots of equation (64) are negative.

To study the stability of the fixed points corresponding to Case (a), we let $p_1 = p_2 = q_1 = q_2 = 0$ in equation (64) and obtain the eigenvalues

$$\lambda = \mu_1 \pm i\nu_1,\ -\mu_3 \pm i\nu_3,\ -\mu_2 \pm \sqrt{a_3^2 - \nu_2^2}\,. \tag{65}$$

Hence, the fixed points corresponding to Case (a) are asymptotically stable if and only if

$$a_3^2 < \mu_2^2 + \nu_2^2 \tag{66}$$

where $a_n^2 = p_n^2 + q_n^2$.

To study the stability of the fixed points corresponding to Case (b), we let $p_1 = q_1 = 0$ in equation (64) and obtain the two roots

$$\lambda = -\mu_1 \pm \sqrt{a_2^2 - \nu_1^2} \tag{67}$$

and four roots governed by the characteristic equation

$$\begin{vmatrix} \lambda+\mu_2+q_3 & \nu_2-p_3 & -q_2 & p_2 \\ -\nu_2-p_3 & \lambda+\mu_2-q_3 & -p_2 & -q_2 \\ 2\Gamma q_2 & 2\Gamma p_2 & \lambda+\mu_3 & \nu_3 \\ -2\Gamma p_2 & 2\Gamma q_2 & -\nu_3 & \lambda+\mu_3 \end{vmatrix} = 0 . \tag{68}$$

Again, the fixed points in this case are asymptotically stable if and only if the real parts of all the eigenvalues in equations (67) and (68) are negative.

5. Numerical Results for Fixed-Point Solutions

To show the effect of varying the detunings and the excitation amplitude on the fixed points for Cases (a), (b), and (c), we let $\Gamma = 0.625$, $\mu_1 = \mu_2 = 0.5$, and $\mu_3 = 0.1$. In all of the figures, continuous lines represent stable solutions (sinks), dotted lines represent unstable solutions with positive real eigenvalues (saddles), and dashed lines represent unstable solutions with a complex conjugate pair of eigenvalues having a positive real part (unstable foci).

In Figure 1, we show the effect of varying the excitation amplitude F on the response amplitudes a_1 (Figure 1a), a_2 (Figure 1b), and a_3 (Figure 1c). Here, we set $\sigma = \sigma_2 = 0.5$ and $\sigma_3 = 0.0$. The solution corresponding to Case (b) exists when $F > F_1 \approx 0.275$ (Figures 1b and 1c). When $F_1 < F < F_2 \approx 0.284$, Case (b) is double-valued, with the small solution (saddle) being unstable with a positive real eigenvalue and the large solution (sink) being stable (Figure 1b). We note that at F_1 there is a fold or saddle-node bifurcation whereas at F_2 there is a reverse pitchfork bifurcation. The solution corresponding to Case (c) exists when $F > F_3 \approx 0.323$. When $0 < F < F_1$, only the solution corresponding to Case (a) exists and is stable (Figures 1b and 1c). Hence, the response in this case is periodic consisting of the third mode only. When $F_1 < F < F_2$, three

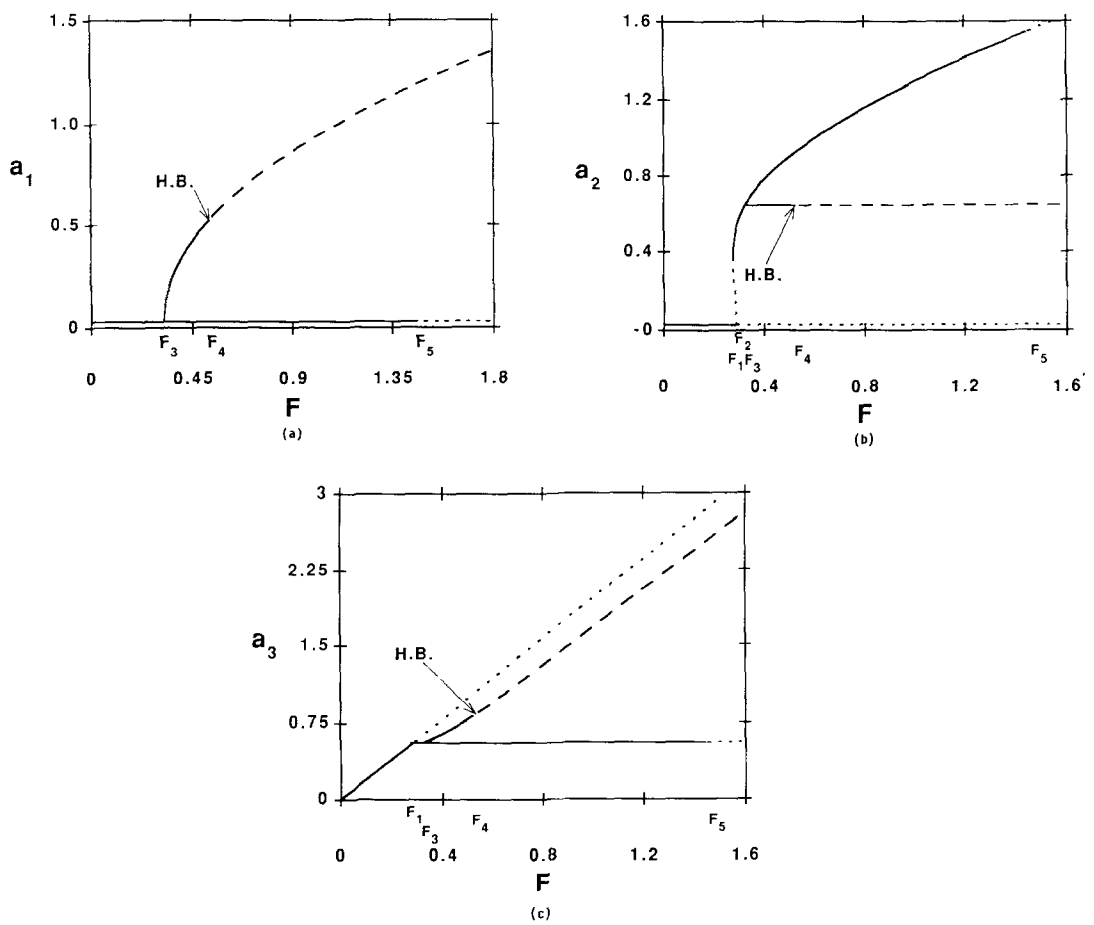

Fig. 1. Force-response curves: (a) first mode, (b) second mode, and (c) third mode. (. . .) Unstable with a positive real eigenvalue, (---) unstable with a pair of complex conjugate eigenvalues lying in the right half plane, and (___) stable. Here, $\sigma = 0.5$, $\sigma_2 = 0.5$, $\sigma_3 = 0.0$, $\mu_1 = 0.5$, $\mu_2 = 0.5$, $\mu_3 = 0.1$, and $\Gamma = 0.625$.

solutions exist: a solution corresponding to Case (a), which is stable: a solution corresponding to Case (b), which is stable; and a solution corresponding to Case (b), which is unstable with a positive real eigenvalue (saddle) (Figures 1b and 1c). Here, the response is periodic consisting of either the third mode only or the second and third modes. When $F_2 < F < F_3$, there are two possible solutions: a solution corresponding to Case (a), which is unstable with a positive real eigenvalue, and a solution corresponding to Case (b), which is stable (Figures 1a and 1c). Here, the response is periodic consisting of the second and third modes. When $F_3 < F < F_4 \approx 0.528$, three possible solutions exist: a solution corresponding to Case (a), which is unstable with a positive real eigenvalue; a solution corresponding to Case (b), which is stable; and a solution corresponding to Case (c), which is stable. In this case, the response is periodic consisting of either the second and third modes or all three modes. When $F_4 < F < F_5 \approx 1.444$, three possible solutions exist: a solution corresponding to Case (a), which is unstable with a positive real eigenvalue (saddle); a solution corresponding to Case (b), which is stable (sink); and a solution corresponding to Case (c), which is unstable (unstable focus) with the real part of a pair of complex conjugate eigenvalues being positive. Here, the response of the three-degree-of-freedom system is either a periodic motion consisting of the second and third modes or an amplitude- and phase-modulated motion consisting of all three modes. We note that at F_4 there is a Hopf bifurcation. When $F > F_5$, there are three possible solutions: a solution corresponding to Case (a), which is unstable with a positive real eigenvalue (saddle); a solution corresponding to Case (b), which is also unstable with a positive real eigenvalue (saddle); and a solution corresponding to Case (c), which is unstable (focus) with the real part of a pair of complex conjugate eigenvalues being positive. Here, the response is an amplitude- and phase-modulated motion consisting of all three modes.

In many nonlinear systems the response depends on the sweep direction. As we sweep the excitation amplitude up from $F = 0$, we begin with the solution corresponding to Case (a), which is stable. Hence, the response is periodic and consists of only the third mode. The amplitude a_3 of the third mode, the directly excited mode, increases linearly with F until F reaches the critical value F_2. When F is increased beyond F_2 (Figure 1b), the fixed-point solution corresponding to Case (a) becomes unstable with a positive real eigenvalue. Hence, the response jumps up to the solution corresponding to Case (b), which is stable. Here the response is a two-mode periodic response with the second and third modes present. As F is increased further, the amplitude a_3 of the excited mode remains constant (saturates), independent of F (Figure 1c), and is given by equation (42). As F is increased beyond F_5, Case (b) becomes unstable with a positive real eigenvalue, and the response jumps to the solution corresponding to Case (c), where a fixed point of the modulation equations is unstable with the real part of a pair of complex conjugate eigenvalues being positive. Here, the response is an amplitude- and phase-modulated motion consisting of all three modes.

As we sweep F down from say $F > 2.5$, at first the solution corresponds to Case (c), where a fixed point of the modulation equations is unstable with a pair of complex conjugate eigenvalues lying in the right-half of the complex plane, and the response is an amplitude- and phase-modulated motion. As F is decreased, the response remains an amplitude- and phase-modulated motion until F reaches the critical value F_4. As F is decreased below the Hopf bifurcation point F_4, the solution corresponding to Case (c) becomes stable, and hence the response becomes periodic consisting of all three modes. The response of the overall system remains periodic consisting of all three modes until F is decreased below F_3 where the solution corresponding to Case (c) ceases and the response latches onto the solution corresponding to Case (b). Hence, the

response is periodic consisting of the second and third modes. As F is decreased below F_1 the solution corresponding to Case (b) ceases (Figures 1b and 1c), and the response jumps down to the solution corresponding to Case (a), which is periodic consisting of the third mode only. The overhang region between F_1 and F_2 corresponds to a subcritical instability. In this interval, the response may correspond to either Case (a) or Case (b), depending on the initial conditions.

In Figure 2, we show variations of the amplitudes a_1 (Figure 2a), a_2 (Figure 2b), and a_3 (Figures 2c, 3) with σ. Here, we set $F = 0.5$, $\sigma_2 = 0.5$, and $\sigma_3 = 0.0$. When $\sigma < \sigma^{(1)} \approx -0.909$ or $\sigma > \sigma^{(10)} \approx 0.909$, only solution a is possible and it is stable (Figures 2b and 2c). The response in this case is periodic consisting of the third mode only (essentially a linear response). Solution b exists when σ is between $\sigma^{(1)}$ and $\sigma^{(10)}$. When $\sigma^{(1)} < \sigma < \sigma^{(3)} \approx -0.782$ or $0.781 \approx \sigma^{(7)} < \sigma < \sigma^{(10)}$, Case (b) is double-valued: the smaller solution is unstable with a real eigenvalue being positive and the larger solution is stable (Figure 2b). The values $\sigma^{(1)}$ and $\sigma^{(10)}$ correspond to saddle-node bifurcations, whereas $\sigma^{(3)}$ and $\sigma^{(7)}$ correspond to reverse pitchfork bifurcations. When $\sigma^{(1)} < \sigma < \sigma^{(2)} \approx -0.858$ or $0.902 \approx \sigma^{(9)} < \sigma < \sigma^{(10)}$, there are two possible solutions: a solution corresponding to Case (a), which is stable, and a solution corresponding to Case (b), which is also stable (Figure 3). Here the response is periodic consisting of either the third mode only or the second and third modes. The values $\sigma^{(2)}$ and $\sigma^{(9)}$ correspond to branch bifurcations.

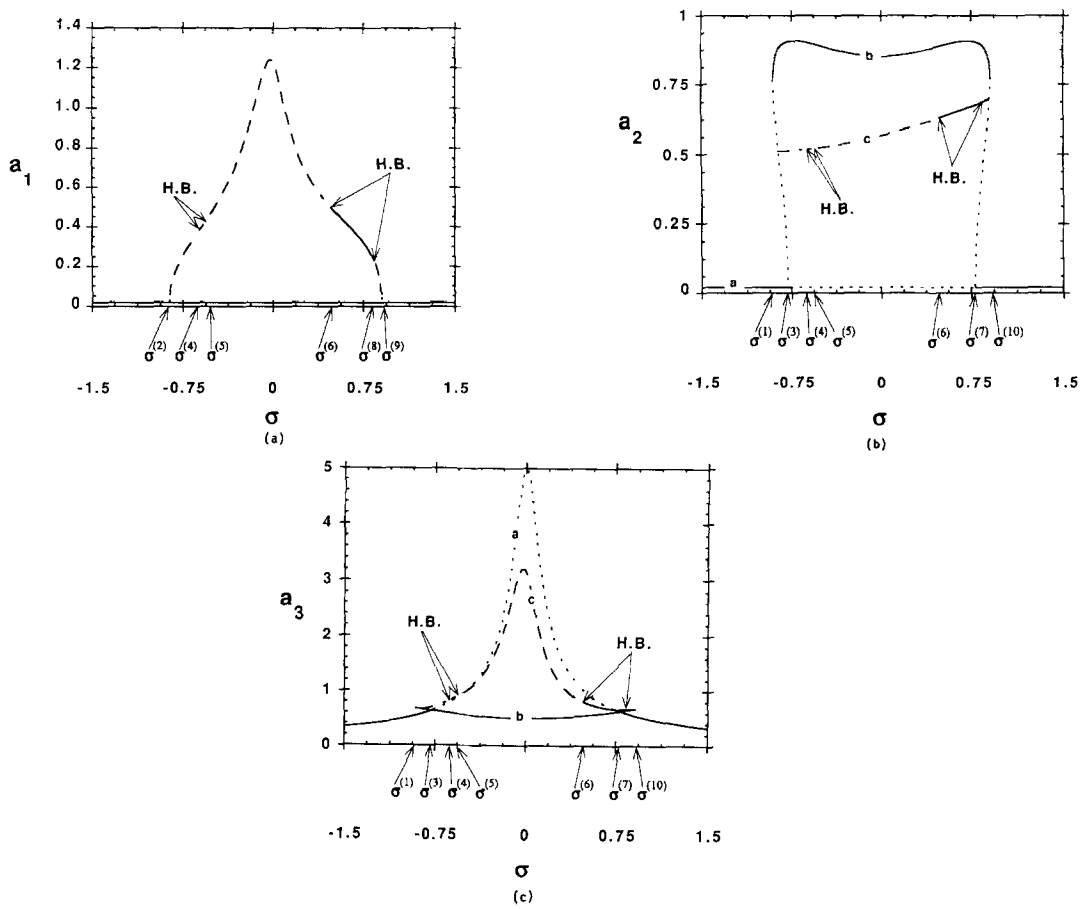

Fig. 2. Frequency-response curves: (a) first mode, (b) second mode, and (c) third mode. (. . .) Unstable with a positive real eigenvalue, (---) unstable with a pair of complex conjugate eigenvalues lying in the right half plane, and (___) stable. Here, $F = 0.5$, $\sigma_2 = 0.5$, $\sigma_3 = 0.0$, $\mu_1 = 0.5$, $\mu_2 = 0.5$, $\mu_3 = 0.1$, and $\Gamma = 0.625$.

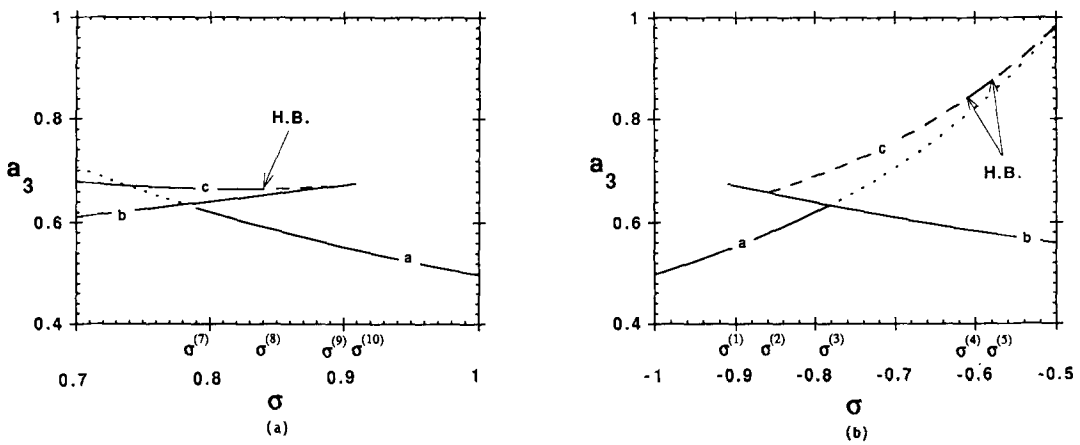

Fig. 3. Expanded portions of the frequency-response curves for the third mode. (. . .) unstable with a positive real eigenvalue, (---) unstable with a pair of complex conjugate eigenvalues lying in the right half plane, and (___) stable. Here, $F = 0.5$, $\sigma_2 = 0.5$, $\sigma_3 = 0.0$, $\mu_1 = 0.5$, $\mu_2 = 0.5$, $\mu_3 = 0.1$, and $\Gamma = 0.625$.

When $\sigma^{(2)} < \sigma < \sigma^{(3)}$ or $0.844 \approx \sigma^{(8)} < \sigma < \sigma^{(9)}$, there are three possible solutions: a fixed-point solution corresponding to Case (a), which is stable; a solution corresponding to Case (b), which is stable; and a solution corresponding to Case (c), which is unstable with the real part of a pair of complex conjugate eigenvalues being positive (Figure 3). Here, the response can be periodic consisting of the third mode only, or periodic consisting of the second and third modes, or an amplitude- and phase-modulated motion consisting of all three modes. When $\sigma^{(3)} < \sigma < \sigma^{(4)} \approx -0.571$ or $-0.474 \approx \sigma^{(5)} < \sigma < \sigma^{(6)} \approx 0.473$, there are three possible solutions: a solution corresponding to Case (a), which is unstable with a real eigenvalue being positive; a solution corresponding to Case (b), which is stable; and a solution corresponding to Case (c), which is unstable with the real part of a pair of complex conjungate eigenvalues being positive (Figure 2c and 3a). Hence, the response consists of either a periodic solution consisting of the second and third modes or an amplitude- and phase-modulated motion consisting of all three modes. When $\sigma^{(4)} < \sigma < \sigma^{(5)}$ or $\sigma^{(6)} < \sigma < \sigma^{(7)}$, three solutions exist: a solution corresponding to Case (a), which is unstable with a real eigenvalue being positive; a solution corresponding to Case (b), which is stable; and a solution corresponding to Case (c), which is stable (Figures 2 and 3). In this case, the response is periodic consisting of either the second and third modes or all three modes. When $\sigma^{(7)} < \sigma < \sigma^{(8)}$, three stable solutions exist: a solution corresponding to Case (a); a solution corresponding to Case (b); and a solution corresponding to Case (c). Hence in this case, the response is periodic consisting of the third mode only, the second and third modes only, or all three modes. We note that there are Hopf bifurcations at $\sigma^{(4)}$, $\sigma^{(5)}$, $\sigma^{(6)}$, and $\sigma^{(8)}$.

As we slowly sweep σ upwards from $\sigma = -1.5$, at first the solution corresponds to Case (a) ($a_1 = a_2 = 0$) (Figures 2b, 2c, 3b), and the response is periodic consisting of the third mode only. It remains stable until σ reaches the critical value $\sigma^{(3)}$. As σ is increased beyond $\sigma^{(3)}$, the solution corresponding to Case (a) loses stability with one real eigenvalue becoming positive, and the response jumps to that corresponding to either Case (b) or Case (c). In the first case, a_1 remains zero, a_3 decreases slightly, and a_2 jumps up from zero to a large value. As σ is increased further, the response stays locked onto the solution corresponding to Case (b), which is periodic and consists of the second and third modes, until σ reaches the critical value $\sigma^{(10)}$, where the solution for Case (b) ceases (Figures 5, 6, 8). As σ is increased beyond $\sigma^{(10)}$, the response jumps down to the solution corresponding to Case (a). If at $\sigma = \sigma^{(3)}$ the response jumps to that corresponding to

Case (c), it becomes an amplitude- and phase-modulated motion consisting of all three modes. It remains aperiodic (it may even become chaotic) until σ exceeds $\sigma^{(4)}$, where the fixed points of the modulation equations undergo a reverse Hopf bifurcation, and the response becomes periodic consisting of all three modes. As σ is increased beyond $\sigma^{(5)}$, the fixed points undergo a Hopf bifurcation and the response becomes an amplitude- and phase-modulated motion. As σ is increased beyond $\sigma^{(6)}$, the fixed points undergo another reverse Hopf bifurcation and the response becomes periodic again and remains so until σ reaches $\sigma^{(8)}$. When σ exceeds $\sigma^{(8)}$, the fixed points undergo another Hopf bifurcation and again the response becomes an amplitude- and phase-modulated motion. As σ is increased beyond $\sigma^{(9)}$, solution c ceases and the response jumps to the solution corresponding to either Case (b) or Case (a).

As we slowly sweep σ down from $\sigma = 1.5$, the response is periodic corresponding to Case (a). It remains stable until σ is decreased below $\sigma^{(7)}$, where the corresponding fixed point loses stability with a real eigenvalue becoming positive, and the response jumps to either a periodic motion consisting of the second and third modes, corresponding to Case (b), or a periodic motion consisting of all three modes, corresponding to Case (c). In the first case, the response remains stable until σ is decreased below $\sigma^{(1)}$, where a_2 jumps down to zero whereas a_3 jumps down to the solution corresponding to Case (a). If at $\sigma = \sigma^{(7)}$, the response jumps to the solution corresponding to Case (c), it will be periodic consisting of all three modes. As σ is decreased further the response will remain until σ reaches the value $\sigma^{(6)}$, where the fixed points exhibit a loss of stability due to a Hopf bifurcation and the response becomes an amplitude- and phase-modulated motion consisting of all three modes. As σ is decreased below $\sigma^{(5)}$, the fixed points undergo a reverse Hopf bifurcation and the response becomes periodic again. The response remains periodic until σ is decreased below $\sigma^{(4)}$, where the fixed points undergo a Hopf bifurcation, and the response becomes an amplitude- and phase-modulated motion consisting of all three modes. The response remains modulated until σ is decreased below $\sigma^{(2)}$ where the solution for Case (c) ceases and the response jumps to that corresponding to either Case (a) or Case (b).

6. Modulated Motions

As discussed in Sections 3 and 5, the fixed points of the modulation equations (21)–(27) or (52)–(57) correspond to periodic solutions of (1)–(3). Moreover, for some excitation and system parameters, the fixed-point solutions of the modulation equations may undergo Hopf bifurcations. Near these Hopf bifurcations, the modulation equations possess limit-cycle solutions, which correspond to either two-period quasiperiodic or phase-locked solutions of (1)–(3), depending on whether the frequency of the limit cycle is commensurate or incommensurate with Ω. To locate these limit cycles, we use the *shooting* method described by Aprille and Trick [42]. To determine the stability of these limit cycles and the bifurcations that they may undergo, we use Floquet theory [13]. Once these limit-cycle solutions of equations (52)–(57) lose stability and are no longer periodic, we resort to the use of Poincaré sections and fast Fourier transforms (FFT) to discern the nature of the ensuing bifurcations. In this study, we observed that for some excitation and system parameters the p_i and q_i become two-period quasiperiodic (i.e., motion on a T^2 torus). The two-period quasiperiodic solution of the modulation equations becomes synchronous (frequency locked) in which the ratio of its two basic frequencies is an integer. As F is increased further, there is a torus breakdown [43], leading to a chaotic solution of the modulation equations, and hence the motion becomes chaotically modulated.

6.1. *Limit Cycles of the Modulation Equations*

As discussed in Section 4, at the point $F = F_4$ in Figure 1 there is a Hopf bifurcation. Near this bifurcation, the modulation equations possess limit-cycle solutions. Using the aforementioned algorithms, we calculated some of these limit cycles and investigated their bifurcations.

As F is increased past F_4, we first obtain a period-one solution. In Figure 4, we show a typical period-one limit-cycle solution obtained when $F = 0.530$. In Figures 4a, b, and c, we show three projections of the limit cycle. For this system we see that a period-one solution consists basically of a single loop in space, in this case a six-dimensional space. The Poincaré section consists of a single point. The cross-section for this construction is the hyperplane $q_1 = -0.667p_1 + 0.560$. The FFT of p_1 is shown in Figure 4d; it consists of a single basic frequency and its harmonics. In all cases presented in this section, the time record used to calculate the FFT corresponds to 9,000 one-sided intersections with the Poincaré cross-section.

As F is increased further this limit-cycle solution remains stable until F is nearly equal to 0.531, where one of the Floquet multipliers leaves the unit circle through -1. Hence, the solution is expected to undergo a period-doubling bifurcation. In Figure 5, we show a typical period-doubled limit cycle obtained when $F = 0.533$. In Figures 5a, b, and c, we show three projections of the limit cycle. The double loops indicate a period-doubled limit cycle. The Poincaré section contains two distinct points, confirming the period-doubling of the limit cycle. In Figure 5d, we show the FFT of the period-two solution. When this FFT is compared to that of the period-one solution in Figure 4d, we can see that there are distinct peaks midway between the previous peaks.

6.2. *Quasiperiodic Solutions*

The period-doubled solution remains stable until F reaches approximately 0.5366 where a complex-conjugate pair of Floquet multipliers crosses the unit circle. When this occurs the solution is no longer periodic; instead it becomes quasiperiodic. This type of bifurcation is sometimes referred to as a secondary Hopf or Niemark bifurcation.

In Figures 6–8, we show a typical two-period quasiperiodic solution (i.e., motion on a T^2 torus) obtained when $F = 0.537$. In Figure 6, we show three projections of motion on a torus. Unlike the trajectories of the previous limit-cycle solutions, the trajectory in this case does not close. When these projections are viewed in real time, they appear as tumbling versions of the limit cycles. In Figure 7a, we show the FFT of this solution. At a first glance it appears to have a broadband character, which is characteristic of a chaotic motion. However, when a portion is expanded (Figure 7b), we see that it consists of discrete peaks. These peaks are located at values which are combinations of the two basic frequencies of the quasiperiodic motion. In Figure 8, we show a one-sided Poincaré section of this solution. The cross-section chosen for this construction is the plane $q_1 = -0.667p_1 + 0.560$. This hyperplane is transverse to the trajectory generated by the system of modulation equations. Here, the section consists of closed loops, which indicate the presence of two basic frequencies; that is, the solution is two-period quasiperiodic. There are two loops because the chosen section cuts the torus at two locations.

The two-period quasiperiodic motion breaks down as F is increased past $F = 0.53719$. The motion then becomes synchronous with the ratio of the two basic frequencies becoming an integer. In Figures 9–11, we show a typical frequency-locked solution when $F = 0.5372$. The phase space (Figure 9) closely resembles that of the quasiperiodic solution. However, when it is viewed in real time in the phase space, the orbit no longer tumbles. The peaks in the FFT of Figure 10 are

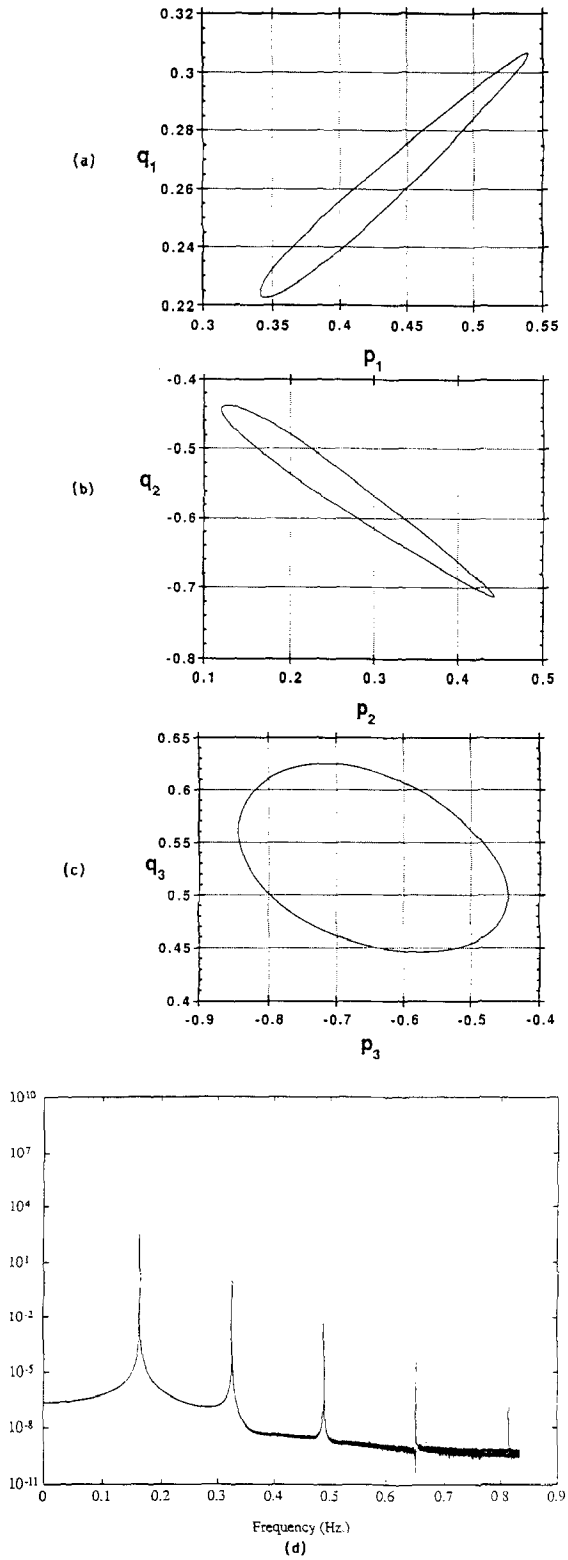

Fig. 4. A typical period-one limit-cycle when $F = 0.530$: (a, b, and c) two-dimensional projections and (d) the FFT of p_1.

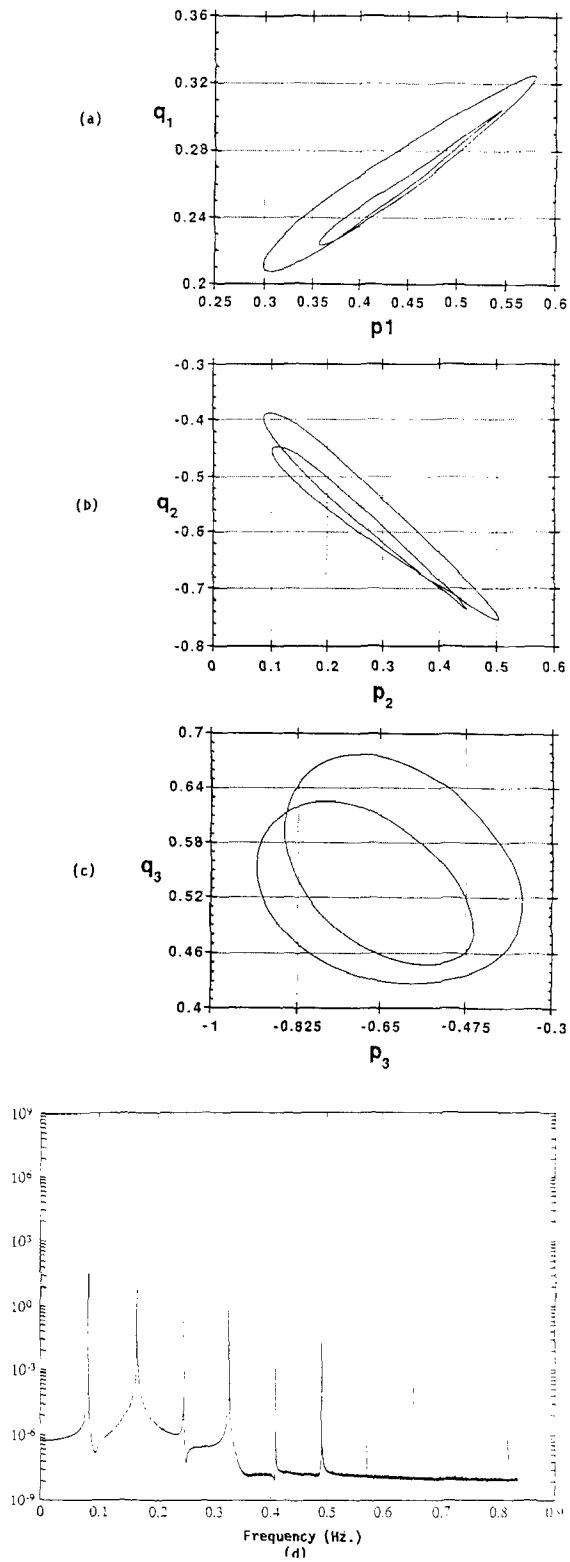

Fig. 5. A typical period-two limit cycle when $F = 0.533$: (a, b, and c) two-dimensional projections and (d) the FFT of p_1.

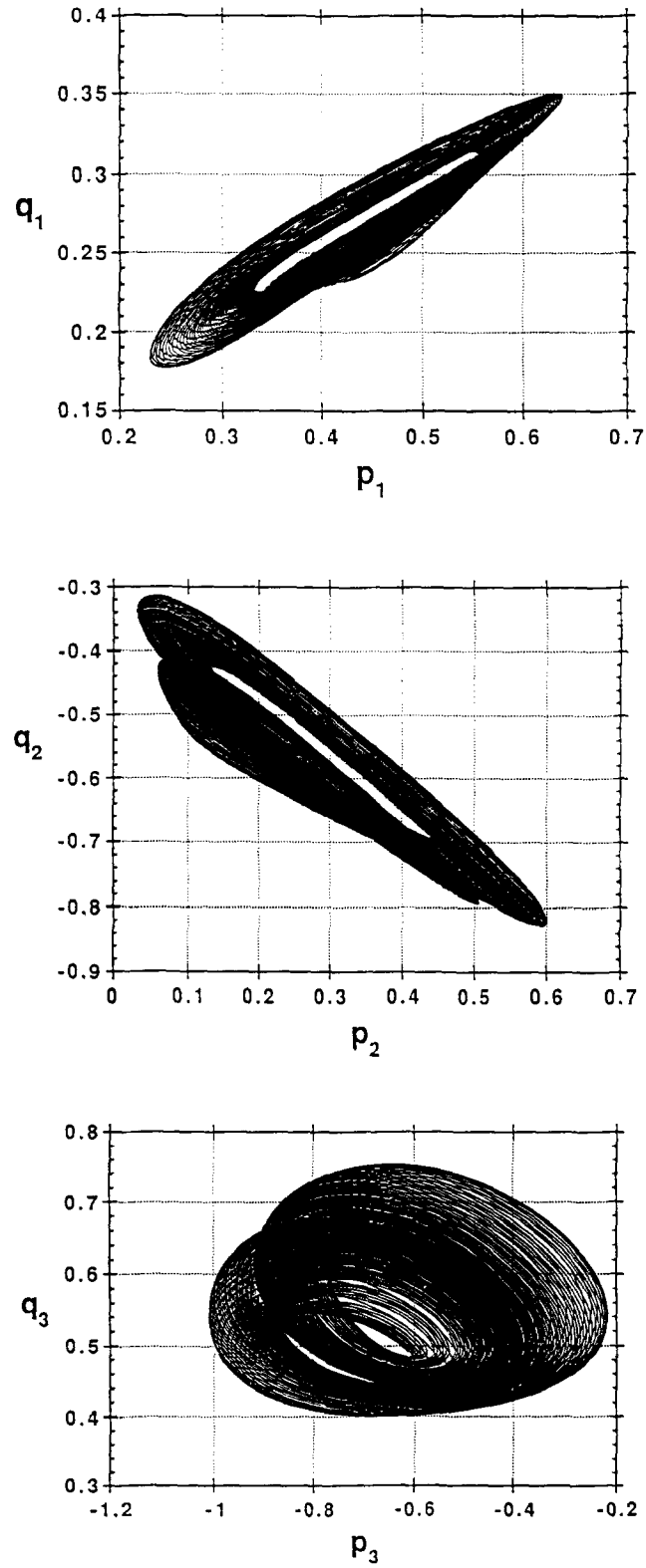

Fig. 6. Three two-dimensional projections of a typical quasiperiodic solution when $F = 0.537$

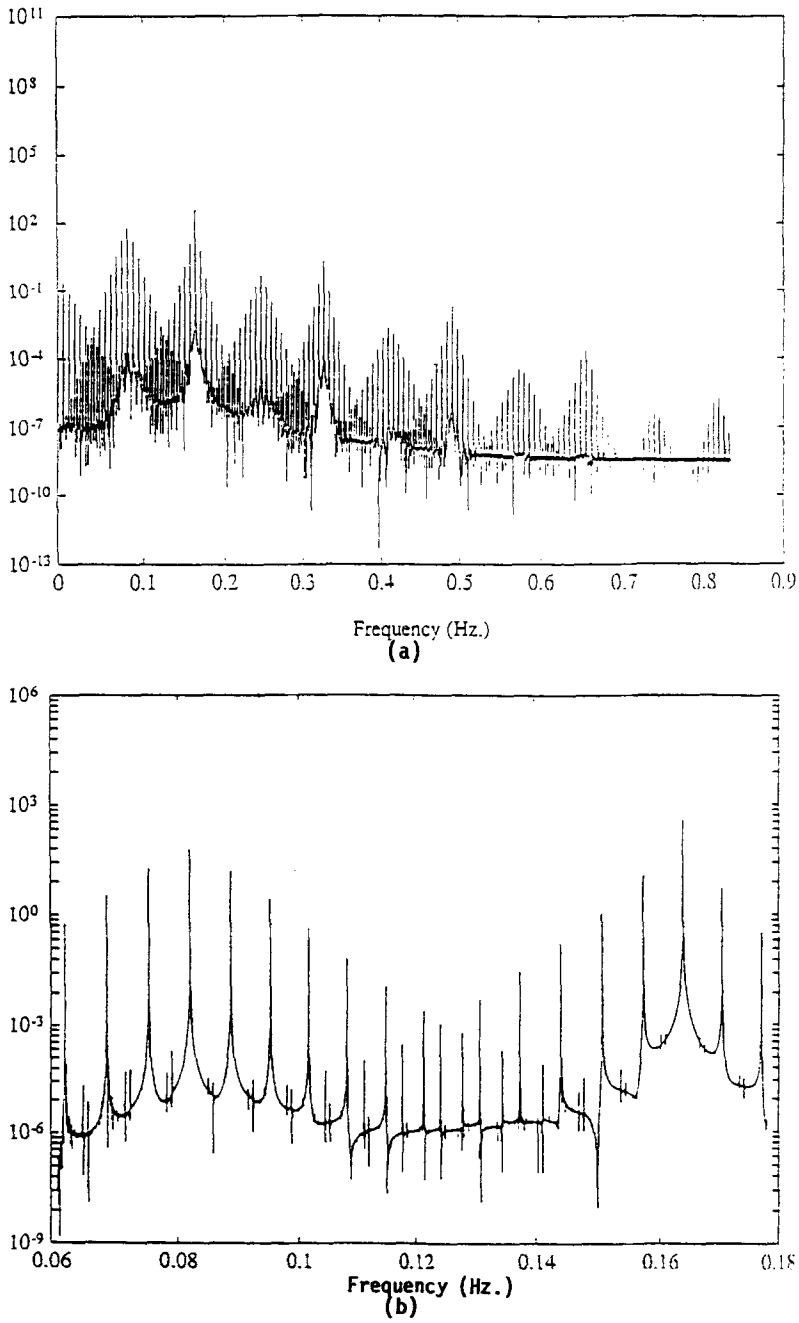

Fig. 7. (a) The FFT of p_1 for a typical quasiperiodic solution when $F = 0.537$ and (b) an expanded portion of this FFT.

shifted to the right, indicating a shift in at least one of the basic frequencies. The difference between the quasiperiodic and frequency-locked solutions is most apparent in the Poincaré sections. In Figure 11, the Poincaré section contains a loosely spaced finite number of points. The section for the quasiperiodic solution (Figure 8) consists of densely packed points which lie on a closed curve.

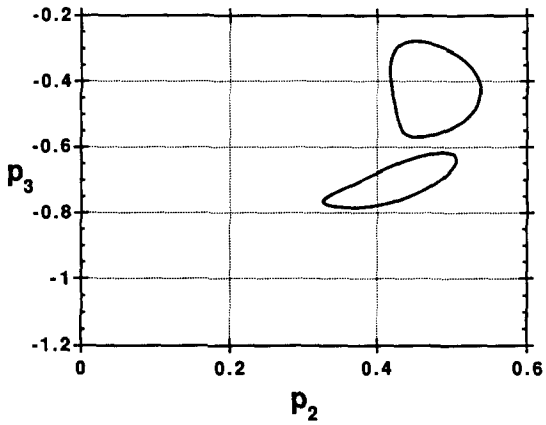

Fig. 8. A projection of the Poincaré section of a typical quasiperiodic solution onto the $p_3 - p_2$ plane when $F = 0.537$

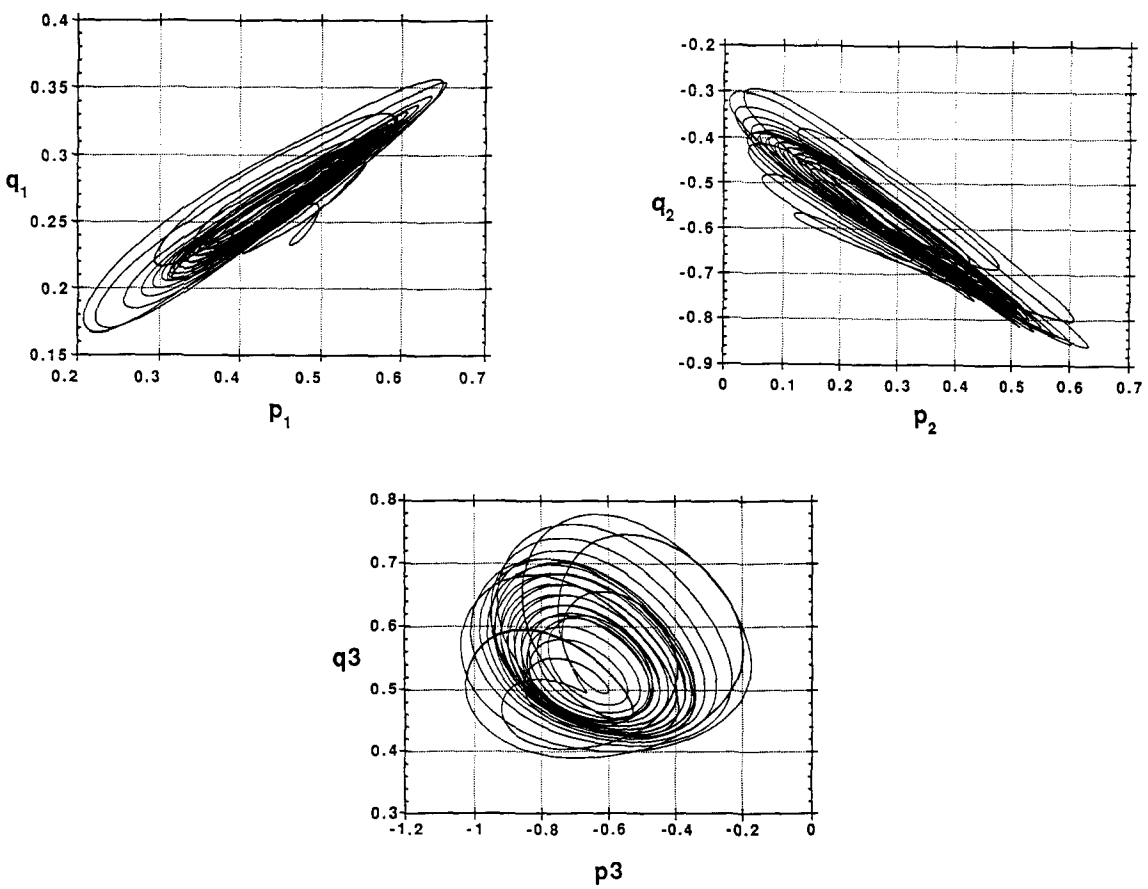

Fig. 9. Three two-dimensional projections of a typical synchronous solution when $F = 0.5372$.

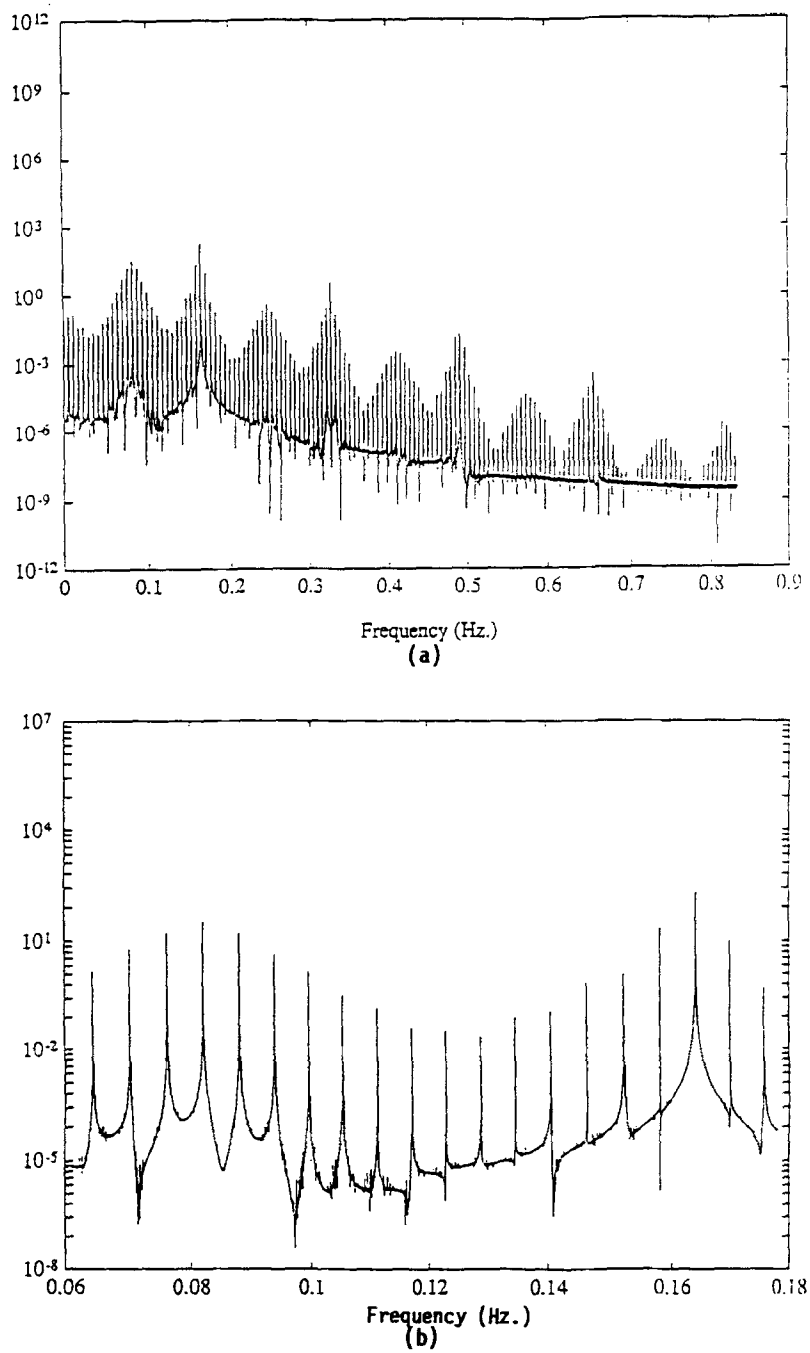

Fig. 10. (a) The FFT of p_1 for a typical synchronous solution when $F = 0.5372$ and (b) an expanded portion of this FFT.

The frequency-locked solution remains stable until $F \approx 0.539$ where it becomes chaotic. In Figures 12–14, we show a typical chaotic solution. A portion of the phase space (Figure 12) is almost completely filled up. The FFT (Figure 13) of p_1 shows an obvious broadband structure. The Poincaré section (Figure 14) consists of points that do not repeat and do not have a definite structure. We attempted to confirm the chaotic nature of this attractor by calculating the

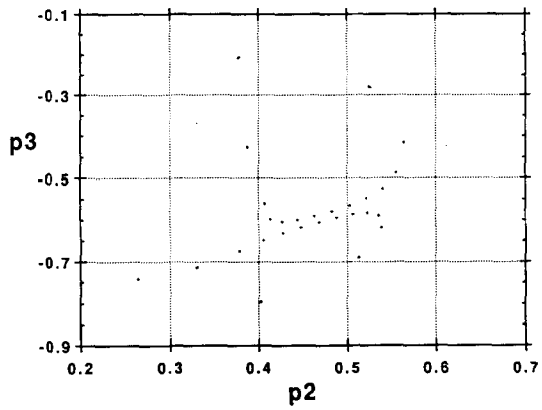

Fig. 11. A projection of the Poincaré section of a typical synchronous solution onto the $p_3 - p_2$ plane when $F = 0.5372$: there are 9000 points in this section.

Lyapunov exponents and hence its Lyapunov dimension. However, this attractor is close to the value of F at which bifurcation from the frequency-locked solution to the chaotic solution took place. Consequently, we were unable to discern the change in the sign of one of the exponents from negative to positive because three of the exponents are very small.

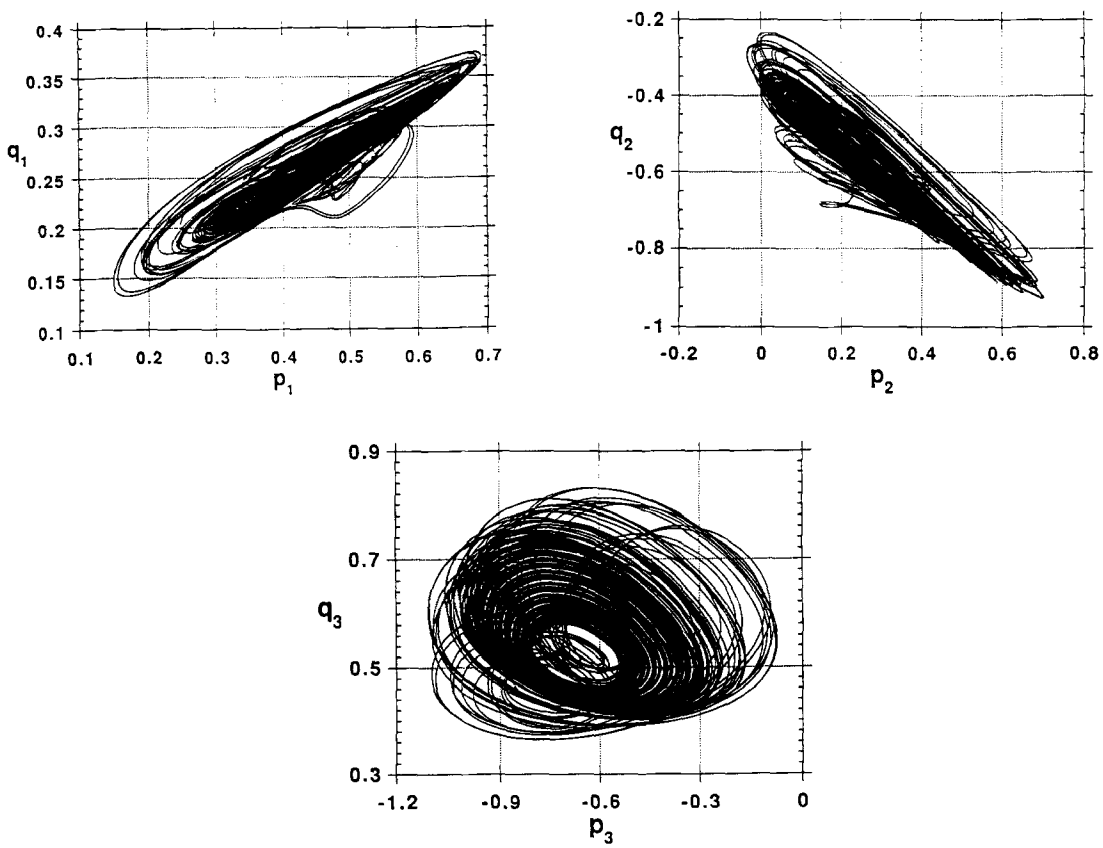

Fig. 12. Three two-dimensional projections of a typical chaotic solution when $F = 0.539$.

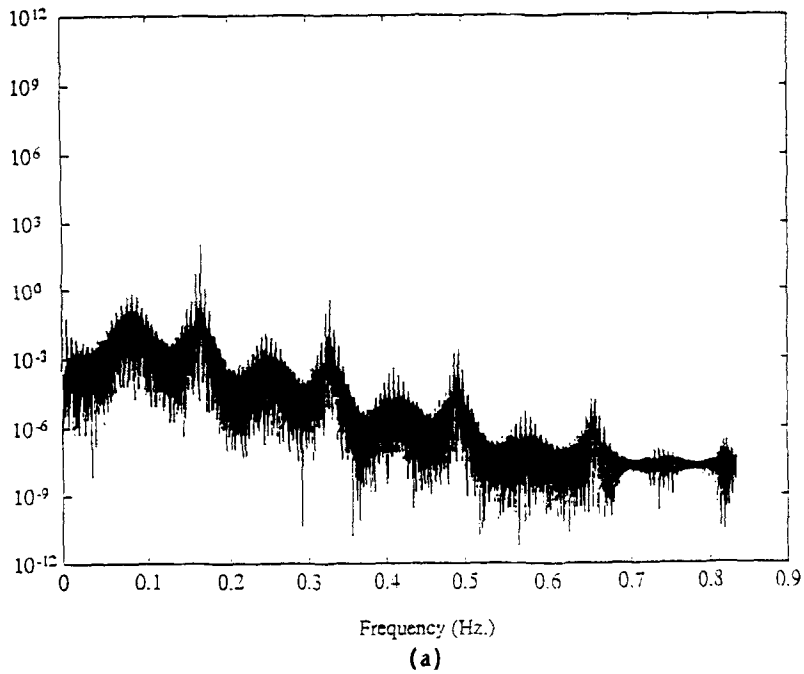

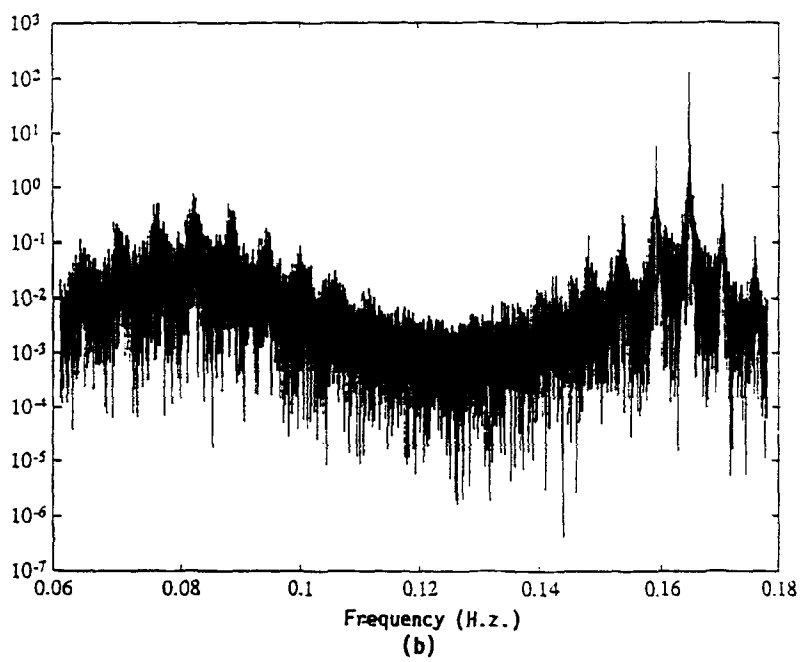

Fig. 13. (a) The FFT of p_1 for a typical chaotic solution when $F = 0.539$ and (b) an expanded portion of this FFT.

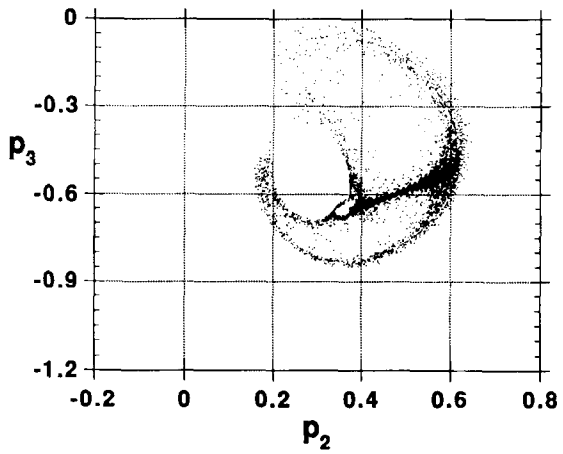

Fig. 14. A projection of the Poincaré section of a typical chaotic solution onto the $p_3 - p_2$ plane when $F = 0.539$: there are 9000 points in this section.

7. Concluding Remarks

We study the response of a general three-degree-of-freedom system with the internal resonant conditions $\omega_3 \approx 2\omega_2 \approx 4\omega_1$ to a primary resonant excitation of the third mode. The method of multiple time scales is used to obtain the amplitude- and phase-modulation equations. We determine the fixed-point solutions of these equations and their stability. These fixed points undergo Hopf bifurcations and hence the modulation equations possess limit-cycle solutions near these bifurcations. The limit-cycle solutions undergo a period-doubling bifurcation. Then, the resulting limit cycle undergoes a secondary Hopf bifurcation, resulting in a two-period quasiperiodic solution, which becomes phase-locked and then eventually breaks down into chaos.

Due to the internal resonance, excitation of the third mode (propellers) can induce large responses in the second (wing) and first (rudder) modes. Thus, the present analysis qualitatively explains the transfer of energy from the propellers to the wing and the rudder, which may be responsible for the breakup of the airplane described by Lefschetz [1].

Acknowledgement

This work was supported by the Army Research Office under Grant No. DAAL03-89-K-0180. The authors greatly appreciate the comments and suggestions of Dr. B. Balachandran.

References

1. Lefschetz, S., 'Linear and nonlinear oscillations', in E. F. Beckenback (ed.), *Modern Mathematics for the Engineer*, McGraw-Hill, New York, 1956, 7–30.
2. Nayfeh, A. H., 'Application of the method of multiple scales to nonlinearly coupled oscillators', in J. O. Hirschfelder, R. E. Wyatt, and R. D. Coalson (eds.), *Lasers, Molecules and Methods*, John Wiley and Sons, New York, 1989, 137–196.
3. Nayfeh, A. H. and Balachandran, B., 'Modal interactions in dynamical and structural systems', *Applied Mechanics Reviews* **42**, 1989, 175–201.

4. Froude, W., 'Remarks on Mr. Scott-Russell's paper on rolling', *Transactions of the Institute of Naval Architects* **4**, 1863, 232–275.
5. Mettler, E. and Weidenhammer, F., 'Zum problem des kinetischen durchschlangens schwack gekrümmter Stäbe', *Ingenieur Archiv* **31**, 1962, 421–432.
6. Sethna, P. R., 'Vibration of dynamical systems with quadratic nonlinearities', *Journal of Applied Mechanics* **32**, 1965, 576–582.
7. Haxton, R. S. and Barr, A. D. S., 'The autoparametric vibration absorber', *Journal of Engineering Industry* **94**, 1972, 119–125.
8. Nayfeh, A. H., Mook, D. T., and Marshall, L. R., 'Nonlinear coupling of pitch and roll modes in ship motions', *Journal of Hydronautics* **7**, 1973, 145–152.
9. Nayfeh, A. H., *Perturbation Methods*, Wiley-Interscience, New York, 1973.
10. Nayfeh, A. H., *Introduction to Perturbation Techniques*, Wiley-Interscience, New York, 1981.
11. Yamamoto, T. and Yasuda, K., 'On the internal resonance in a nonlinear two-degree-of-freedom system (forced vibrations near the lower resonance point when the natural frequencies are in the ratio 1:2)', *Bulletin of the Japan Society of Mechanical Engineers* **20**, 1977, 169–175.
12. Yamamoto, T., Yasuda, K., and Nagasaka, I., 'On the internal resonance in a nonlinear two-degree-of-freedom system (forced vibrations near the higher resonance point when the natural frequencies are in the ratio 1:2)', *Bulletin of the Japan Society of Mechanical Engineers* **20**, 1977, 1093–1101.
13. Nayfeh, A. H. and Mook, D. T., *Nonlinear Oscillations*, Wiley-Interscience, New York, 1979.
14. Hatwal, H., Mallik, A. K., and Ghosh, A., 'Nonlinear vibrations of a harmonically excited autoparametric system', *Journal of Sound and Vibration* **81**, 1982, 153–164.
15. Miles, J. W., 'Resonantly forced motion of two quadratically coupled oscillators', *Physica D* **13**, 1984, 247–260.
16. Nayfeh, A. H. and Raouf, R. A., 'Nonlinear oscillation of circular cylindrical shells', *International Journal of Solids and Structures* **23**, 1987, 1625–1638.
17. Nayfeh, A. H. and Raouf, R. A., 'Nonlinear forced response of infinitely long circular cylindrical shells', *Journal of Applied Mechanics* **54**, 1987, 571–577.
18. Nayfeh, A. H., 'On the undesirable roll characteristics of ships in regular seas', *Journal of Ship Research* **20**, 1988, 92–100.
19. Hatwal, H., Mallik, A. K., and Ghosh, A., 'Forced nonlinear oscillations of an autoparametric system – part 2: chaotic motions', *Journal of Applied Mechanics* **50**, 1983, 663–668.
20. Haddow, A. G., Barr, A. D. S., and Mook, D. T., 'Theoretical and experimental study of modal interaction in a two-degree-of-freedom structure', *Journal of Sound and Vibration* **97**, 1984, 451–473.
21. Nayfeh, A. H. and Zavodney, L. D., 'Experimental observation of amplitude- and phase-modulated responses of two internally coupled oscillators to a harmonic excitation', *Journal of Applied Mechanics* **55**, 1988, 706–710.
22. Nayfeh, A. H., Balachandran, B., Colbert, M. A., and Nayfeh, M. A., 'An experimental investigation of complicated responses of a two-degree-of-freedom structure', *Journal of Applied Mechanics* **56**, 1989, 960–967.
23. Nayfeh, A. H. and Balachandran, B., 'Experimental investigation of resonantly forced oscillations of a two-degree-of-freedom structure', *International Journal of Non-Linear Mechanics* **25**, 1990, 199–209.
24. Balachandran, B. and Nayfeh, A. H., 'Nonlinear oscillations of a harmonically excited composite structure', *Composite Structures* **16**, 1990, 323–339.
25. Balachandran, B. and Nayfeh, A. H., 'Nonlinear motions of a beam-mass structure', *Nonlinear Dynamics* **1**, 1990, 39–61.
26. Mook, D. T., Marshall, L. R., and Nayfeh, A. H., 'Subharmonic and superharmonic resonances in the pitch and roll modes of ship motions', *Journal of Hydronautics* **8**, 1974, 32–40.
27. Mook, D. T., HaQuang, N., and Plaut, R. H., 'The influence of an internal resonance on nonlinear structural vibrations under combination resonance conditions', *Journal of Sound and Vibration* **104**, 1983, 229–241.
28. Mook, D. T., Plaut, R. H., and HaQuang, N., 'The influence of an internal resonance on non-linear structural vibrations under subharmonic resonance conditions', *Journal of Sound and Vibration* **102**, 1985, 473–492.
29. Balachandran, B. and Nayfeh, A. H., 'Observations of modal interactions in resonantly forced beam-mass structures', *Nonlinear Dynamics* **2**, 1991, 77–117.
30. Nayfeh, A. H. and Mook, D. T., 'A saturation phenomenon in the forced response of systems with quadratic nonlinearities', *Proceedings of 8th International Conference on Nonlinear Oscillations*, September 11–15, 1978, Prague, Czechoslovakia, pp. 511–516.
31. Ibrahim, R. A. and Barr, A. D. S., 'Autoparametric resonance in a structure containing a liquid, part II: three mode interaction', *Journal of Sound and Vibration* **42**, 1975, 181–200.
32. Ibrahim, R. A., Woodall, T. D., and Heo, H., 'Modal analysis of structural systems involving nonlinear coupling', *The Shock and Vibration Bulletin* **54**, 1984, 19–27.
33. Bux, S. L. and Roberts, J. W., 'Non-linear vibratory interactions in systems of coupled beams', *Journal of Sound and Vibration* **104**, 1986, 497–520.

34. Nayfeh, T. A., Nayfeh, A. H., and Mook, D. T., 'A theoretical-experimental investigation of a three-degree-of-freedom structure', AIAA Paper No. 90-1081, 1990.
35. Ashworth, R. P. and Barr, A. D. S., 'The resonances of structures with quadratic inertial non-linearity under direct and parametric harmonic excitation', *Journal of Sound and Vibration* **118**, 1987, 47–68.
36. Sridhar, S., Mook, D. T., and Nayfeh, A. H., 'Non-linear resonances in the forced responses of plates, part I: symmetric responses of circular plates', *Journal of Sound and Vibration* **41**, 1975, 359–373.
37. Hadian, J. and Nayfeh, A. H., 'Modal interaction in circular plates', *Journal of Sound and Vibration* **142**, 1990, 279–292.
38. Cartmell, M. P. and Roberts, J. W., 'Simultaneous combination resonances in an autoparametrically resonant system', *Journal of Sound and Vibration* **123**, 1988, 81–101.
39. Fujino, Y., Pacheco, B. M., and Warnitchai, P., 'An experimental and analytical study of autoparametric resonance in a 3DOF model of cable-stayed-beam', *Nonlinear Dynamics*, submitted for publication.
40. Ibrahim, G.M., *The Response of Three-Degree-of-Freedom Systems with Quadratic Nonlinearities to a Harmonic Excitation*. Master's thesis, Jordan University of Science and Technology, December 1986.
41. Tadjbakhsh, I. G. and Wang Y., 'Wind-driven nonlinear oscillations of cables', *Nonlinear Dynamics* **1**, 1990, 265–291.
42. Aprille, T. J. and Trick, T. N., 'A computer algorithm to determine the steady-state response of nonlinear oscillators', *IEEE Transactions on Circuit Theory* CT-19, 1972, 354–360.
43. Berge, P., Pomeau, X., and Vidal, C., *Order within Chaos – Towards a Deterministic Approach to Turbulence*, John Wiley and Sons, New York, 1984.